forests

MDPI

Article

Potential Westward Spread of Emerald Ash Borer, *Agrilus planipennis* Fairmaire, 1888 (Coleoptera: Buprestidae) from Eastern Ukraine

Valentyna Meshkova [1,2,*], Oleksandr Borysenko [3,4], Tetiana Kucheryavenko [5], Yuriy Skrylnyk [2], Kateryna Davydenko [2,6] and Jaroslav Holusa [1]

1 Faculty of Forestry and Wood Sciences, Czech University of Life Sciences Prague, Kamýcká 1283, 16500 Prague-Suchdol, Czech Republic; holusa@fld.czu.cz
2 Department of Entomology, Phytopathology, and Physiology, Ukrainian Research Institute of Forestry & Forest Melioration, Pushkinska 86, UA-61024 Kharkiv, Ukraine; yuriy.skrylnik@gmail.com (Y.S.); kateryna.davydenko74@gmail.com (K.D.)
3 Department of Geoinformation Technologies and Space Monitoring of the Earth, National Aerospace University «Kharkiv Aviation Institute», Chkalov Street 17, UA-61070 Kharkiv, Ukraine; xalekter@gmail.com
4 Department of Remote Sensing, Tartu Observatory, University of Tartu, EE-61602 Toravere, Estonia
5 State Specialized Forest Protection Enterprise "Kharkivlisozahyst", Kharkiv District, Pokotylivka, Str. Nezalezhnosti, 127, UA-62458 Kharkiv, Ukraine; tanya_kucheryavenko@ukr.net
6 Department of Forest Mycology and Plant Pathology, Swedish University of Agricultural Sciences, P.O. Box 7026, SE-75007 Uppsala, Sweden
* Correspondence: valentynameshkova@gmail.com or meshkova@fld.czu.cz

Abstract: Emerald ash borer (EAB), *Agrilus planipennis*, is a phloem-boring beetle, native to East Asia that has become a serious invasive pest of ash (*Fraxinus* spp.) trees in North America and European Russia since the early 2000s. In 2019, EAB was detected in Ukraine. It had spread over 300 km from the entry point over two years and killed hundreds of *Fraxinus excelsior* and *F. pennsylvanica* trees. EAB poses a threat to the ash forests of neighboring European countries, which have already been damaged by the invasive fungus *Hymenoscyphus fraxineus*. The purpose of this research was (i) to reveal the traits of EAB and the climatic variables that affect its survival; (ii) to predict the EAB expansion range in Ukraine and westward; and (iii) to compare the most significant bioclimatic variables in the native, invasive ranges of EAB, as well as outside these ranges. The results demonstrated the following: (i) in all ranges, EAB has adapted to the seasonal temperature variations; (ii) the MaxEnt model predicted the potential distribution of EAB with high accuracy (AUC = 0.988); the predicted area of EAB invasion covered 87%, 48%, and 32% in Luhansk, Kharkiv, and Donetsk regions, respectively; and (iii) the ranges of climatic variables in EAB-inhabited regions demonstrated the high ecological plasticity of this pest. However, the predictions could be improved by considering forest structure, as well as the localization of roads.

Keywords: emerald ash borer; *Fraxinus* spp.; seasonal development; bioclimatic variables; MaxEnt

Citation: Meshkova, V.; Borysenko, O.; Kucheryavenko, T.; Skrylnyk, Y.; Davydenko, K.; Holusa, J. Potential Westward Spread of Emerald Ash Borer, *Agrilus planipennis* Fairmaire, 1888 (Coleoptera: Buprestidae) from Eastern Ukraine. *Forests* **2023**, *14*, 736. https://doi.org/10.3390/f14040736

Academic Editor: Chiara Ferracini

Received: 15 January 2023
Revised: 21 March 2023
Accepted: 30 March 2023
Published: 3 April 2023

1. Introduction

The native range of Emerald ash borer (EAB) (*Agrilus planipennis* Fairmaire, 1888) (Coleoptera: Buprestidae) comprises temperate Northeast Asia, including some areas of China, Japan, South Korea, as well as the Primorsky and Khabarovsky Krais of Russia [1,2]. In these areas, it has colonized native ash species (*Fraxinus mandshurica* Rupr. and *F. chinensis* Roxb.) but has not caused significant damage [3,4].

The invasive range of EAB was developed almost simultaneously on two continents. In North America, EAB was first recorded in 2002 in the Midwestern U.S. (Detroit, Michigan) and in neighboring Canada (Windsor, Ontario) [5,6], and in 2003, it was recorded in the European portion of Russia in the urban stands in Moscow [2,7,8]. However, EAB likely existed undetected in North America and European Russia since the 1990s.

In subsequent years, EAB spread across North America in the west and north regions [2], and across the European continent, north to Tver and St. Petersburg [9,10] and south to Azov [11,12] and Krasnodar Krai [13]. In contrast to North America where EAB spread over forests, in Russia, it settled in urban stands and roadside shelter belts of *F. pennsylvanica* [14,15].

In Ukraine (in the Luhansk Region), EAB was found in 2019 [16,17]. However, judging by the presence of the different larval instars and exit holes, it likely invaded the region in 2017, or potentially earlier, probably from the neighboring Voronezh region of Russia. In 2021, EAB spread throughout the Luhansk region and into the Kharkiv region [18,19]. The data on EAB distribution in 2022 were unavailable due to this region being involved in active hostilities.

After identifying EAB in North America, where this beetle killed millions of ash trees [20] and caused great economic losses, this pest has attracted much attention from researchers. Hundreds of publications have been devoted to EAB detection by modeling the possible spread and threat to ash stands [2,4,6]. Concerns about EAB spread in Europe increased when it was found that EAB infested various native and exotic ash species [1,5,18,21,22], in particular, *F. excelsior*, which was the most common in Europe among all ash species [23]. In recent decades, over a large area in Europe, *F. excelsior* has been damaged by ash dieback caused by the fungus *Hymenoscyphus fraxineus* [24–26]. Amid the increased frequency of droughts, *F. excelsior* was noticeably damaged by foliage and stem pests [22], and due to a decrease in the groundwater levels and the weakening of the root systems, root-rot has spread [26]. All of this could increase the susceptibility of *F. excelsior* to EAB attacks [22].

It was found that the rate of active spread of EAB from its invasion points was significantly lower than the passive points via transport vehicles, or "hitchhiking" [10,27,28]. Therefore, several models have been developed to predict EAB spread that considered the probability of this pest being transported from the point of its current location to a specific distant destination. For example, Prasad et al. [29] described a spatially explicit cell-based model used to calculate the risk of EAB spread in Ohio by combining its flight and short-range dispersal ("insect flight") with human-facilitated, long-range dispersal ("insect ride").

Yemshanov et al. [30,31] and Orlova-Bienkowskaja and Bieńkowski [15] considered pairwise distances between all locations of EAB presence as the main parameter determining the probability of pest spread. Flø et al. [32] considered import pathways of deciduous wood chips in Europe to predict the potential distribution areas for EAB and three more *Agrilus* beetles.

At the same time, the ability of an alien species to survive in a new territory depends on climatic conditions [11,12,33], the presence of host trees [2], and competing or entomophagous species [34,35]. Therefore, EAB spread was predicted according to climatic conditions [11,12,36–39], the spread of the host plant [21,40], landscape characteristics [27], and various combinations of approaches. For example, Webb et al. [37], when studying the potential rapidity of EAB spread in Great Britain, used two approaches: the observed rate of EAB spread in North American and Russian regions; and the relationship between the accumulated degree days and pest emergence that could determine environmental suitability and the EAB life cycle.

Within the current range, EAB has a 1-year or a 2-year cycle [41–43]. The threat to tree health was less in the regions with a 2-year cycle due to slower population growth [4]. Eggs, larvae, and pupae of EAB developed under the bark, where they were protected from extreme weather [44]. EAB adults left the tree in late spring–early summer, feeding on ash foliage for a week before mating and two weeks after mating [2–5,20,43,45–53]. Since the microclimate of individual stands and even stem parts could vary within the same forest, the instar composition of overwintering larvae and the timing of adult emergence could also differ [41,42,54]. Therefore, in order to predict the potential distribution of EAB outside

the current range, it was necessary to analyze the features of the seasonal development of the pest in native and invasive ranges.

To predict the potential distribution area, the species distribution models (SDMs) based on the present data of a plant or animal with the relevant environmental variables have frequently been used [32,38,39,55–59]. The maximum entropy (MaxEnt) model has the possibility of obtaining relatively high accuracy in its predictions [60–62] when considering predictors such as temperature and rainfall at different times of the year [63].

Although climatic factors alone may be insufficient as insect distribution predictors in specific cases [21,32,38,39,64], in a preliminary analysis of the environmental suitability of EAB in Ukraine and its neighboring European countries, we used bioclimatic variables [63]. At the same time, we also considered that both *F. excelsior* and *F. pennsylvanica* were present in this area of the forest and in protective plantations, in particular, those located on roadsides [23,57]. We speculated that for the successful spread of EAB, in addition to the presence of ash, its proportion in forest stands and their microclimates must be considered, which depended on many stand characteristics, such as their fragmentation and density. These issues will be addressed in a future study in the territory, for which all the necessary data will be made available.

The purpose of this research was (i) to compare the traits of EAB's seasonal development in different ranges and to reveal the climatic variables that could affect its survival; (ii) to predict the EAB expansion range in Ukraine and westward; and (iii) to compare the most significant parameters outside of the current EAB range with those in the native and invasive ranges.

2. Materials and Methods

2.1. EAB Phenology and Importance of Climatic Parameters

Data for points with EAB presence in Asia, North America, and Europe (European part of Russia and Ukraine) (Table S1) were compiled from databases and articles [11,12,18,19,22,65,66] and our unpublished field data for 2021. The EAB seasonal development was analyzed using published data from different regions [2–5,20,41,43,45–53] and our own data for the three years of EAB presence in Ukraine [18,19,54,67], as well as comparisons with another *Agrilus* species, particularly *Agrilus biguttatus* (Fabricius, 1776) [68–70].

For detailed characteristics, 12 points were chosen (Table 1). For each of these points, mean monthly air temperature and precipitation were used (Table S2), and additional climatic parameters were evaluated. Among these points, the seasonal development of EAB was studied in detail in three points from China [3,43], three points from the U.S. [41,45], one point from the Russian Federation [42], and one point from Ukraine [54,67]. Two more points (Kharkiv and Luhansk, Ukraine) were chosen because EAB had been found in respective administrative regions. Lviv (Ukraine) and Prague (Czech Republic) were chosen because they are located at almost the same latitude as Kharkiv but westward. The daily air temperature was sourced from the ERA5-Land Global Atmospheric Reanalysis dataset [71]. Annual growing degree days (AGDD) for a base temperature of 10 °C (AGDD10) [11], annual mean temperature, and growing season temperature were calculated for the aforementioned 12 points (Table 1).

We chose the Köppen–Geiger climate classification [72] to characterize both native and invasive ranges of EAB because it was based on the empirical relationship between climate and vegetation. According to this classification, there were five main climate groups: A (tropical), B (arid), C (temperate), D (continental), and E (polar). In each group, there were subgroups by seasonal precipitation (for example, w—dry winter, f—no dry season, s—dry summer) and by temperature (for example, a—hot summer, b—warm summer, c—cold summer). Therefore, Dfa denoted a hot-summer humid continental climate and Dfb indicated a warm-summer humid continental climate. The Köppen–Geiger climate type [72] was determined for each range's most northern, southern, western, and eastern points using ClimateCharts [73].

Table 1. Characteristics of the points for which climatic variables were analyzed in detail.

Point, Country	EAB Is Detected, Predicted, or Not Predicted	Continent	Latitude	Longitude	Climate Type by Köppen–Geiger [73]
Changchun, China	detected	Asia	43.88	125.23	Dwa
Harbin, China	detected	Asia	45.75	126.77	Dwa
Tianjin, China	detected	Asia	39.03	117.20	Cwa
Cincinnati, U.S.	detected	North America	39.10	−84.42	Cfa
Michigan, U.S.	detected	North America	42.22	−83.11	Dfa
Texas, U.S.	detected	North America	32.00	−102.08	BSh
Moscow, Russian Federation	detected	Europe	55.75	37.62	Dfb
Svatove, Ukraine	detected	Europe	49.42	38.16	Dfa
Kharkiv, Ukraine	predicted	Europe	50.00	36.25	Dfb
Luhansk, Ukraine	predicted	Europe	48.44	39.34	Dfa
Lviv, Ukraine	not predicted	Europe	49.80	24.00	Cfb
Prague, Czech Republic	not predicted	Europe	49.99	14.45	Cfb

Mean monthly temperature and precipitation (1989–2019) for the selected points on different continents with EAB presence (with 1-year and 2-year cycles) and absence are provided in Supplementary Table S2. The dates of the stable temperature transition through 10 °C in spring and autumn, as well as the duration of the growing season, were evaluated according to a method by V. Meshkova [74].

2.2. EAB Distribution Model

The geographical distribution of *A. planipennis* was predicted based on the ecological niche model devised in MaxEnt software, version 3.4.4 [75,76] because it accepted the presence-only data and a small number of presence-points [60]. The data on EAB presence in the European part of Russia and Ukraine were used for predicting the potential distribution of EAB in Ukraine and neighboring European countries, covering latitudes from 44.6° N (Sevastopol) to 51.5° N (Chernihiv), and longitudes from 14.5° E (Prague) to 39.3° E (Luhansk). Bioclimatic variables representing annual trends in temperature, precipitation, and climate ranges (Table 2) [63] were evaluated for grid cell at a resolution of 2.5 arc-minutes (approximately 3 km^2) based on interpolations of observed data from 1970 to 2000 and downloaded from the WorldClim database (the version released in January 2020) [77,78].

Table 2. Bioclimatic variables.

Variable	Variable Name	Definition
Bio_1, °C	Mean annual temperature	Annual mean temperature
Bio_2, °C	Mean diurnal range	The average difference between high and low daily temperature
Bio_3, dimensionless	Isothermality	The ratio of the mean diurnal temperature range relative to the seasonal range
Bio_4, °C	Temperature seasonality	Temperature variation over a year by monthly average temperature
Bio_5, °C	Max temperature of the warmest month	Monthly mean of daily high temperatures for the hottest month
Bio_6, °C	Min temperature of the coldest month	Monthly mean of daily low temperatures for the coldest month
Bio_7, °C	Temperature annual range	Bio_07 = Bio_05–Bio_06
Bio_8, °C	Mean temperature of the wettest quarter	Average temperature for the three months with the most precipitation
Bio_9, °C	Mean temperature of the driest quarter	Average temperature for the three months with the least precipitation

Table 2. *Cont.*

Variable	Variable Name	Definition
Bio_10, °C	Mean temperature of the warmest quarter	Average temperature for the three hottest months
Bio_11, °C	Mean temperature of the coldest quarter	Average temperature for the three coldest months
Bio_12, mm	Annual precipitation	Total annual precipitation
Bio_13, mm	Precipitation of the wettest month	Total precipitation for the month with the most precipitation
Bio_14, mm	Precipitation of the driest month	Total precipitation for the month with the least precipitation
Bio_15, fraction	Precipitation seasonality	Precipitation variation over a year by monthly total precipitation
Bio_16, mm	Precipitation of the wettest quarter	Total precipitation for the three months with the most precipitation
Bio_17, mm	Precipitation of the driest quarter	Total precipitation for the three months with the least precipitation
Bio_18, mm	Precipitation of the warmest quarter	Total precipitation for the three hottest months
Bio_19, mm	Precipitation of the coldest quarter	Total precipitation for the three coldest months
Elev, m a.s.l.	Elevation	Elevation (altitude)

All 19 bioclimatic variables from the WorldClim database were used as predictors, and the algorithm chose the most important variables through the default regularization settings. For replicates of the SDMs, the default setting of "cross-validation" was chosen, as it utilized all the available data and, thus, could better use the limited data [76]. The settings used in the MaxEnt models are shown in Table 3.

Table 3. Selected MaxEnt settings.

MaxEnt Option	Selected Setting	MaxEnt Option	Selected Setting
Create response curves	Yes	Write plot data	Yes
Make picture of predictions	Yes	Extrapolate	Yes
Do jackknife to measure variable importance	Yes	Write plots	Yes
Output format	Cloglog	Maximum iterations	1000
Random seed	Yes	Convergence threshold	0.00001
Remove duplicate presence records	Yes	Default prevalence	0.5
Random test percentage	25	Apply threshold rule	Max. test sensitivity plus specificity
Regularization multiplier	1	Logscale raw/ cumulative pictures	Yes
Max number of background points	10,000	Threads	8
Replicates	50	Lq to lqp threshold	80
Replicated run type	Bootstrap	Linear to lq threshold	10
Add samples to background	Yes	Hinge threshold	15

QGIS 3.28.1 was used for converting WorldClim data to ASC format, defining the study area, and building the maps [79].

Model performance was measured using the area under the curve (AUC) parameter of the receiver-operating characteristic (ROC) [80]. AUC was interpreted as the probability of correctly predicting the species presence in a randomly selected geographic grid cell. In the ROC analysis, each grid cell in the predictor dataset received scores from the independent testing dataset; the relationship between the true positive rate and the false positive rate

was plotted; and then, the AUC was calculated. If the AUC of the test data was close to 0.5, the model performed no better than a random model, and if AUC was 1.0, the model provided a perfect fit with no false negatives [76,80]. The influence of different variables on the model was evaluated by contribution and permutation coefficients. As a verification method, we used the jack-knife test, in which three models were generated for each variable: the first one without a variable, the second one with only one, and the third model with all the variables. The results of the calculations are provided in Tables S3 and S4.

2.3. Comparison of the Most Significant Bioclimatic Variables in the New EAB Range with Those in the Native and Invasive Ranges

MaxEnt version 3.4.4 command-line tool [76] was used for acquiring the individual WorldClim data for each point with EAB presence in Asia, North America, and European Russia, as well as for 70 selected points from the territories of the EAB predictions (Table 4).

Table 4. Geographical diversity in native (Asia) and invasive EAB ranges (North America, European Russia, and Ukraine), as well as the area of EAB prediction.

Parameters	EAB Detected			Area for EAB Prediction
	Asia (66 Points)	North America (376 Points)	European Russia and Ukraine (145 Points)	Europe (70 Points)
Latitude, °	24.6–49.4	32.7–49.9	47.1–59.9	44.6–51.5
Longitude, °	115–141.4	−104.8–−63.7	29.8–46.4	14.5–39.3
Elevation, m a.s.l.	2.0–1294.0	9.0–1660.0	−19.0–230.0	10.0–846.0

Note: All points of EAB findings in Asia, North America, European Russia, and Ukraine, as well as 70 selected points from the territory of EAB predictions by our modeling are presented in the supplement (Table S1). In Table 4, the limits for latitude, longitude, and elevation (altitude, m a.s.l.) for these locations are mentioned.

Boxplots representing the ranges of the bioclimatic variables in different ranges of EAB were built using the statistical software package PAST: Paleontological Statistics Software Package for Education and Data Analysis [81].

3. Results

3.1. EAB Phenology

In the native range of EAB in China and in the invasive range in North America, there were populations with 1-year and 2-year cycles. Therefore, in China, EAB had a 1-year development in Tianjin with an average yearly temperature of 13 °C and a 2-year development in Changchun and Harbin with an average yearly temperature of 6 °C and 4.9 °C, respectively [43] (Table 5). In North America, EAB had a 1-year development in the central U.S. (Texas) [41] with an average yearly temperature of 18.7 °C and 2-year development in Cincinnati and Michigan [2,43] with an average yearly temperature of 12.4 °C and 10 °C, respectively (Table 5). With a 1-year life cycle, the fourth instar larva would hibernate once, and with a 2-year life cycle, it would hibernate twice [6,41,43,82].

Table 5. Climatic indicators for several points where EAB was detected, predicted, or not predicted.

Point, Country	EAB Is Detected, Predicted, or Not Predicted	Mean Temperature, °C		Number of Days with T > 10 °C	Number of Months with T > 10 °C	AGDD, Base 10 °C	Date of Stable Transition of Temperature	
		Year	Vegetation Period				over 10 °C	below 10 °C
Changchun, China	detected	6.0	19.6	169	5	1477	23.04	8.10
Harbin, China	detected	4.9	18.6	161	5	1321	27.03	4.10
Tianjin, China *	detected	13.7	21.8	223	7	2519	26.03	3.11
Cincinnati, U.S.	detected	12.4	20.0	212	7	1935	4.04	1.11
Michigan, U.S.	detected	10.0	18.3	186	6	1532	20.04	22.10
Texas, U.S. *	detected	18.7	21.8	293	10	3307	13.02	2.12
Moscow, Russian Federation	detected	6.0	15.9	149	5	899	30.04	25.09
Svatove, Ukraine	detected	8.9	17.8	179	6	1435	15.04	10.10
Kharkiv, Ukraine	predicted	8.8	17.4	177	6	1364	16.04	9.10
Luhansk, Ukraine	predicted	9.4	17.0	182	6	1538	14.04	12.10
Lviv, Ukraine	not predicted	8.6	16.9	174	5	1058	20.04	10.10
Prague, Czech Republic	not predicted	9.6	16.0	181	6	1104	16.04	13.10

Note: Characteristics of the points for which climatic variables were analyzed in detail are presented in Table 1; * the 1-year cycle of EAB.

In the invasive range of this pest in Moscow (Russia) [42] and in Svatove (Ukraine) [54] with an average yearly temperature of 6 °C and 8.9 °C, respectively (Table 5), 2 cohorts developed in EAB populations. The first was represented by individuals that had developed from the earliest laid eggs, reached the fourth instar by the end of the growing season, and, after overwintering, emerged early as adults. The individuals of the second cohort had developed from late-laid eggs, reached the second–third instars by the end of the growing season, and continued their development in the spring. Under favorable conditions, the beetles emerged late in the same year, and under less favorable conditions, they hibernated again as the fourth-instar larvae.

EAB larvae development resumed in spring after the vegetation of the host plant had resumed [54], i.e., after a stable temperature transition above 10 °C, as was typical in other xylophages [69,83,84].

In the east of Ukraine, the ratio of younger and older EAB larvae in October 2019 and March 2020 was approximately the same [54]. It proved that the larvae stopped developing when the dormant period of the host species had begun i.e., after a stable temperature transition below 10 °C. In mid-April, larval molting was registered, and in May, older larvae and prepupa accounted for more than 80% of the individuals [54]. An earlier start and a later end of the growing season were favorable for EAB development [4]. The analysis in Table 5 showed that the AGDD10 at points outside the range of the pest (Lviv, Prague), as well as the average temperatures of the growing season, were no less than in Moscow (invasive range), that is, the lack of heat had not been an obstacle to EAB. These data were consistent with the calculations by Orlova-Bienkowskaja and Bieńkowski [11], according to which the minimal AGDD10s recorded at the locations currently occupied by *A. planipennis* were 714 °C in Asia, 705 °C in North America, and 711 °C in European Russia.

Adult emergence was observed from early May in Tianjin, China [3], and southern Ohio, U.S. [41], from early June in Moscow, Russia [60], from mid-June in central Michigan, U.S. [41,85], and in the Luhansk, Ukraine [67].

Larvae hatching began in June, or later, depending on the time of adult emergence [2,41–43,54]. Larvae fed under the bark until the end of the ash vegetation [41]. Larvae hibernated in their galleries [2,3]. Since the dates of the adult emergence, as well as the dates of all subsequent stages had been extended over time, the larvae were adapted to overwinter at any instar [41,42,67].

A study in North America showed that cold winters could potentially limit the spread of *A. planipennis* in the U.S. and Canada [47]. No established EAB population has been recorded in localities where temperatures below −34 °C occur in Europe [33]. Such temperatures were close to the absolute supercooling point of *A. planipennis* larvae (−35.3 °C) [48]. The climate data analysis showed that such low temperatures were absent in Ukraine and

in other analyzed parts of Europe (see Supplements S1 and S2). Therefore, the potential range of *A. planipennis* in this territory was not limited by too low temperatures.

Sufficient phloem moisture is important for larval development, at an optimum of 60% [86]. In the samples from the east of Ukraine, prepupae had successfully completed development in the branches with a relative phloem humidity of over 30% [54]. The rate of larval development depended on temperature, but it slowed down in trees with better health [50,87], as well as in drying trees with low phloem moisture [54].

In the native range of EAB, a cold winter season was necessary to initiate diapause and adult development [36]. However, in Ukraine, in branch samples collected in October 2019 (average temperature 10 °C) and placed in a laboratory at 15–20 °C, the larvae successfully completed their development, and adults emerged [54]. Since these results had been obtained for only one season, it was necessary to repeat the research at different sampling times.

In choosing bioclimatic variables, we found that in all analyzed points of the three continents, the coldest months were December, January, and February, and the hottest months were June, July, and August (Table S2). Noticeable variations in precipitation throughout the year were revealed by different points. For example, in Changchun, Harbin, and Tianjin with EAB presence and, in Prague, with its absence, the driest months were December, January, and February. In Cincinnati, January, February, and November were the driest months. In Michigan and central regions (North America) with EAB presence and in Lviv with its absence, the driest months were January, February, and March.

In the middle of the U.S., where the growing season lasts 10 months, starting in February, low rainfall during this time was unfavorable for trees, reducing their resistance to pest attacks [88]. In Lviv (Ukraine), where the growing season did not begin until the last third of April, with a significant amount of precipitation in each of its five months (62.5–96.7 mm), the relatively dry first months of the year had not significantly affected the tree health (Table S2). In Moscow, Russia, and eastern Ukraine, the driest months were February, March, and April. The growing season began in the east of Ukraine in mid-April, in Moscow, Russia, two weeks later. At the same time, 690 mm of precipitation per year were in Moscow, and 520 mm in East Ukraine, that is, trees in the latter case were then more susceptible to pests. The wettest in Changchun, Harbin, Tianjin, Moscow, and Prague were summer months (June, July, and August), in Cincinnati and Michigan (April, May, and June), in the central U.S. (July, September, and October), in Svatovo, (June, July, and October) (Table S2). Heavy rainfall in summer was likely unfavorable for EAB adults.

Taking into account the differences in climatic conditions in the EAB ranges and the timing of the seasonal development of this pest, we tested all 19 climatic variables (in Table 2) that were downloaded from the WorldClim dataset for forecasting, using the MaxEnt program [77].

3.2. Maximum Entropy Modeling

MaxEnt predicted the potential distribution of EAB with high model accuracy, resulting in an average test area under the curve (AUC) value of 0.988 and a standard deviation of 0.002 (Tables S3 and S4). The jack-knife test also showed a rather high AUC with each individual variable (Table 6).

Two variables (Bio_4 and Bio_6) had the greatest value in constructing the EAB range model with a cumulated contribution of 66.4%. However, these variables had the highest permutations (see Tables 6 and S3, Figure 1).

Bio_4 showed the variation of temperature over a given year (or averaged years), based on the standard deviation of the monthly temperature averages. The probability of EAB presence increased as Bio_4 approached 1164 (see Figure 1a), the maximum value in the sample points with the presence of this pest. With a further increase in the index, a high permutation was noted (see Table S4). The probability of EAB presence increased as the Bio_6 value increased, up to −10 °C with further high permutations (blue area in Figure 1).

Table 6. Bioclimatic variables with the greatest influence on the MaxEnt probability of EAB presence. Variables are listed in order of descending importance.

Variable Short Name	Variable Description	AUC	Contribution, %	Permutation, %	Cumulated Contribution, %
Bio_4	Temperature seasonality	0.92	46.56	40.88	46.56
Bio_6	Min temperature of the coldest month	0.93	19.87	23.55	66.43
Bio_19	Precipitation of the coldest quarter	0.86	11.16	4.09	77.59
Bio_15	Precipitation seasonality	0.82	10.53	5.63	88.11
Bio_5	Max temperature of the warmest month	0.87	3.73	1.68	91.85
Bio_11	Mean temperature of the coldest quarter	0.93	3.34	2.42	95.19
Bio_9	Mean temperature of the driest quarter	0.83	1.52	0.72	96.70
Bio_8	Mean temperature of the wettest quarter	0.90	0.96	3.70	97.66
elev	Elevation in meters	0.79	0.92	1.69	98.59
Bio_10	Mean temp. of the warmest quarter	0.87	0.48	0.00	99.06
Bio_14	Precipitation of the driest month	0.83	0.23	0.42	99.29
Bio_7	Temperature annual range	0.90	0.20	7.52	99.49
Bio_1	Mean annual temperature	0.87	0.13	5.89	99.62
Bio_3	Isothermality	0.83	0.12	0.94	99.73
Bio_18	Precipitation of the warmest quarter	0.77	0.10	0.76	99.84
Bio_2	Mean diurnal range	0.79	0.09	0.01	99.93
Bio_16	Precipitation of the wettest quarter	0.78	0.04	0.05	99.97
Bio_17	Precipitation of the driest quarter	0.83	0.02	0.05	100.00
Bio_13	Precipitation of the wettest month	0.77	0.00	0.00	100.00
Bio_12	Annual precipitation	0.80	0.00	0.00	100.00

Note: AUC—area under the curve for each variable, a measure of the model's performance.

The contribution of each of Bio_19 and Bio_15 exceeded 10%, and these 4 variables (Bio_4, Bio_6, Bio_19, and Bio_15) contributed 88.11% to the model. The probability of EAB presence increased as Bio_19 increased, to 100 mm, and a further increase in Bio_19 had no effect. The probability of EAB presence reached a maximum at 20% of the variation in precipitation over a year by monthly total precipitation (Bio_15).

The probability of EAB presence reached the maximum at the monthly mean of the daily high temperatures for the hottest month 27 °C (Bio_5) and mean temperatures during the coldest 3 months of the year −6 °C (Bio_11) (see Tables S1 and S2). The contributions of the other variables were low and amounted to about 4% in total (Table 6).

The model showed a high probability in EAB distribution in the eastern region of Ukraine. Climatic conditions were favorable (the probability of EAB spread exceeded 0.5) for its spread in 87% of Luhansk, 48% of Kharkiv, and 32% of Donetsk (Figure 2).

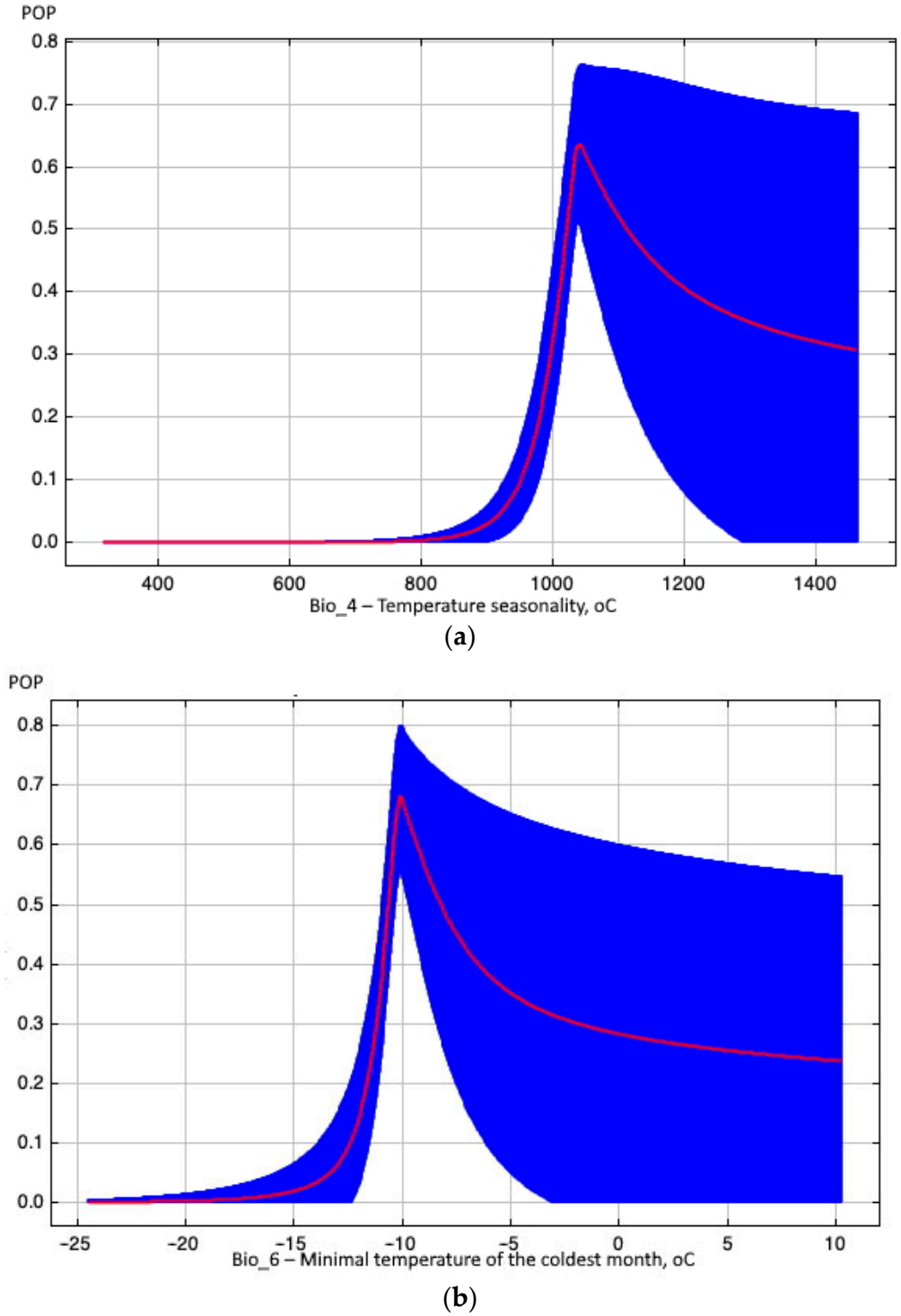

Figure 1. Response curves of bioclimatic variables with the greatest value in constructing the EAB range model. POP—the predicted probability of EAB presence. The curves show how the POP changed as each environmental variable changed, keeping all other environmental variables at their average sample value. The blue area shows the range of POP values when the variable changes. (**a**) Bio_4 (Temperature seasonality); (**b**) Bio_6 (Minimal temperature of the coldest month).

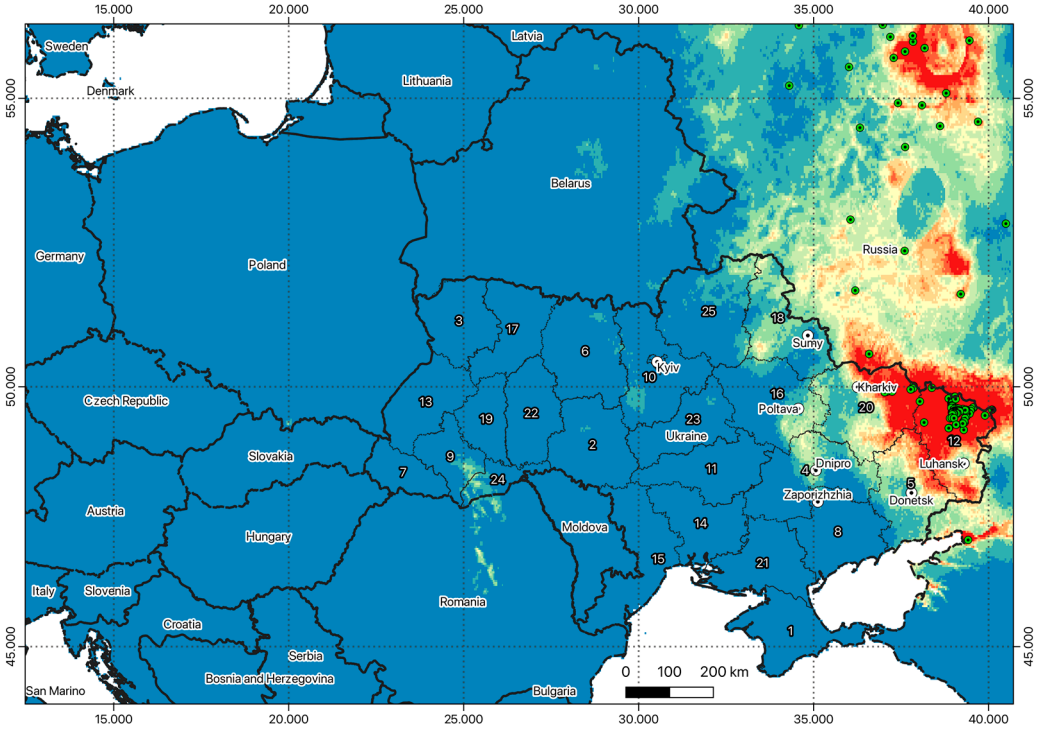

(**a**)

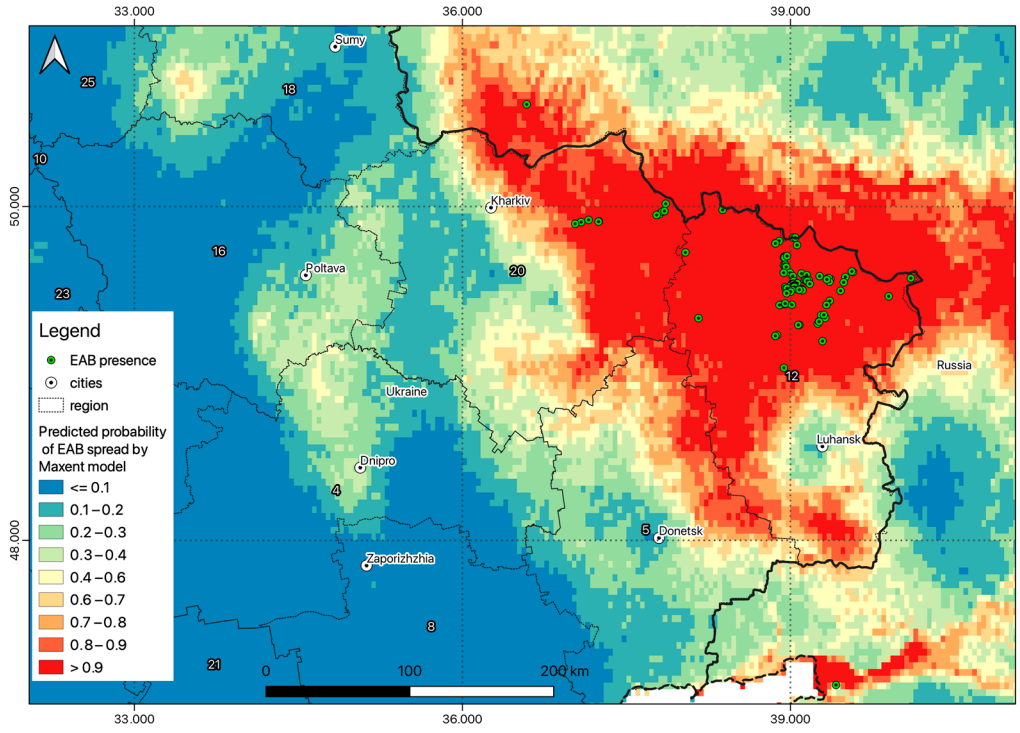

(**b**)

Figure 2. Predicted distribution area for EAB estimated by maximum entropy modeling. (**a**) whole analyzed territory; (**b**) a fragment of the territory with the highest probability of EAB spread. Green circles are points where EAB was detected. Numbers indicate cities and regions of Ukraine: 1—Autonomous Republic of Crimea; 2—Vinnytsia; 3—Volyn; 4—Dnipropetrovsk; 5—Donetsk; 6—Zhytomyr; 7—Zakarpattia; 8—Zaporizhzhia; 9—Ivano-Frankivsk; 10—Kyiv; 11—Kirovohrad; 12—Luhansk; 13—Lviv; 14—Mykolayiv; 15—Odesa; 16—Poltava; 17—Rivne; 18—Sumy; 19—Ternopil; 20—Kharkiv; 21—Kherson; 22—Cherkassy; 23—Chernivtsi; 25—Chernihiv. The color reflects the predicted probability of EAB spread at each grid cell (see the scale in (**b**)).

Less favorable climatic conditions for EAB spread were demonstrated in Sumy, Chernihiv, Kyiv, Zhytomyr, Poltava, Dnipropetrovsk, Cherkasy, and Vinnytsia regions. A rather high probability of possible EAB spread was predicted in Ivano-Frankivsk and Chernivtsi regions of Ukraine, along which a wide band of potential foci continued into Romania, east of the Carpathians, towards Suceava. Another potential focus was predicted in Poland at the border with Slovakia, in the area of the Tatra National Park.

3.3. Bioclimatic Environmental Variables in the Native and Invasive EAB Ranges

As of 2021, the northernmost point of detection was Troitskoe, Russia (49.4° N, Dwb), the southernmost one was Hiroshima, Japan (24.6° N, Cfa), and the easternmost was Shikotsuko, Japan (141.4° E, Dfb). The altitude varied from 2 m a.s.l. (Dongying, China) up to 1294 m a.s.l. (Yangkiaping, China) (Table S1). The invasive ranges of EAB were registered in North America and in European Russia. As of 2021, on the North American continent, the northernmost point of EAB detection was Manitoba (49.9° N, Dfb), the southernmost was Texas (32.7° N, Cfa), the westernmost was Colorado (104.8° W, Cfb), and the easternmost was Nova Scotia (63.7° W, Dfb). The altitude ranged from 9 m a.s.l. (New York) to 1660 m a.s.l. (Colorado) (Table S1).

In the European portion of Russia, the northernmost point of EAB presence was St. Petersburg (59.9° N, Dfb), the most southern one was Azov (47.1° N, Cfa), the most western one was St. Petersburg (29.8° E, Dfb), and the easternmost was Astrakhan (46.4° E, BSk). (Table S1). The altitude varies from −19 m a.s.l. (Astrakhan) up to 230 m a.s.l. (Vyazma) (Table S1).

The territory used to predict the EAB invasion (see Figure 2) covered the whole of Ukraine and part of Central Europe (see Table S1).

Boxplots representing the ranges of the climatic variables in different regions (Figure 3a–f) showed the high ecological plasticity of EAB. The seasonality of temperatures (Bio_4) varied to the greatest extent in the native range, and in the territory of European Russia and Ukraine where EAB was present, Bio_4 was greater than where its presence had not been predicted with climatic data (Figure 3a). At points with EAB presence in European Russia, Bio_4 was from 892.8, in Volgograd, to 1164.1, in St. Petersburg, (Table S1). In Lviv and Prague, where MaxEnt did not predict invasion, this variable was lower (790.2 and 714.5, respectively), but comparable to the value in Texas with EAB presence (Table 7).

Table 7. Bioclimatic variables from MaxEnt for several points where EAB was detected, predicted, or not predicted.

Points	EAB Is Present, Predicted, or Not Predicted	Bio_4	Bio_6	Bio_19	Bio_15	Bio_5	Bio_11
Changchun	detected	1425.2	−23.6	18	106.6	26.8	−14.3
Harbin	detected	1533.5	−25.8	12	111.9	27.1	−16.3
Tianjin *	detected	1098.6	−8.6	14	133.0	30.9	−1.3
Cincinnati	detected	924.2	−6.3	222	16.9	30.4	0.2
Michigan	detected	994.5	−9.8	149	23.0	28.0	−4.0
Texas *	detected	756.7	1.0	322	15.5	33.5	8.1
Moscow	detected	978.7	−10.4	131	31.9	23.2	−6.6
Svatove	detected	1043.2	−10.0	133	19.5	26.6	−5.7
Kharkiv	predicted	1022.5	−8.5	121	22.9	26.8	−4.5
Luhansk	predicted	1018.8	−8.7	116	21.9	27.6	−4.3
Lviv	not predicted	790.2	−6.3	119	38.0	22.9	−2.3
Prague	not predicted	714.5	−4.0	71	46.4	23.7	−0.3

Note: Characteristics of the points for which climatic variables were analyzed in detail are presented in Table 1; *—the 1-year cycle of EAB; Bio_4—Temperature seasonality; Bio_6—Min temp. of the coldest month; Bio_19—Precipitation of the coldest quarter; Bio_15—Precipitation seasonality; Bio_5—Max temp. of the warmest month; Bio_11—Mean temp. of the coldest quarter.

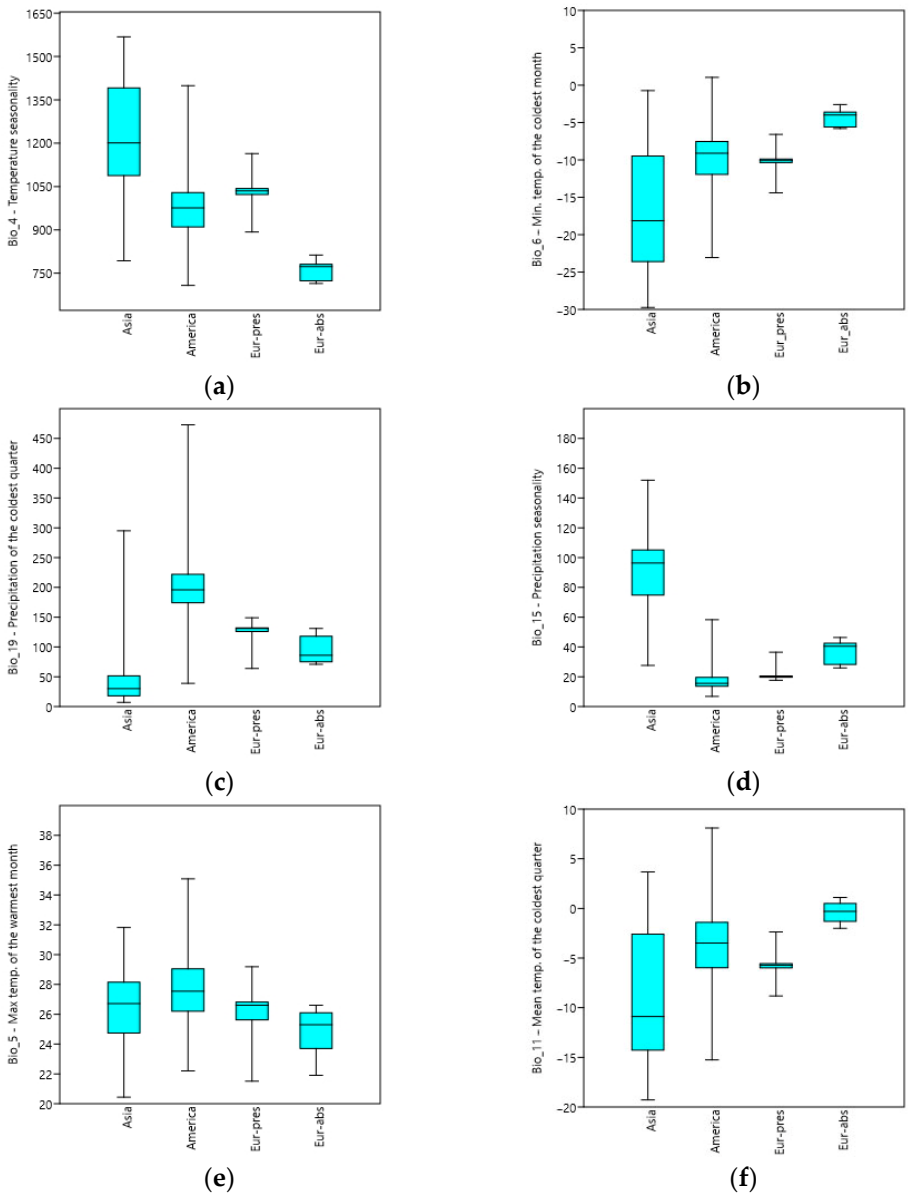

Figure 3. Boxplots representing the ranges of the bioclimatic variables in different regions (Asia, North America, Eur-pres—points with EAB detected in European part of Russia and Ukraine; Eur-abs—points with EAB not predicted in analyzed part of Europe; whisker type—Stand. dev., whisker length—one sigma, quartile method—interpolation); (**a**) Bio_4; (**b**) Bio_6; (**c**) Bio_19; (**d**) Bio_15; (**e**) Bio_5; (**f**) Bio_11.

The minimum temperature of the coldest month (Bio_6) was lower in the native EAB range than in the invasive range; in the territory where EAB presence in Europe had been predicted, it was −11.2–−1.3° C, and in more western regions where it had not been predicted, only −5.8–−2.6 °C (Figure 3b). At points with EAB presence in European Russia, Bio_6 was from −14.4 °C in Michurinsk to −9.1 °C in Azov (Table S1). In Lviv and Prague, where MaxEnt did not predict invasion, this variable was −6.3 °C and −4 °C, respectively, but the same value was mentioned in Cincinnati with EAB presence (Table 7). Bio_6 had the lowest values in the more southern points both in Asia (Tianjin) and in North America (central region), and on the European continent within a close latitude of more western regions, where the climate continentality was less (Lviv, Ukraine, and Prague, Czech Republic)). Precipitation in the coldest quarter of the year (December, January, and February) (Bio_19) was the lowest in EAB locations in Asia, although the maximum value reached almost 300 mm (Figure 3c). In North America, the range of variability in

this variable was wider. In the analyzed areas of Europe, the range of precipitation was narrower than in Asia and North America, but in the areas with EAB presence, the average value was slightly higher than in the areas where its presence had not been predicted (115.5 mm and 95.3 mm, respectively).

At points with EAB presence in European Russia, Bio_19 was from 64 mm in Astrakhan to 149 mm in Azov (Table S1). In other regions where MaxEnt had not predicted invasion, this variable was from 71 mm in Prague to 166 mm in Uzhhorod.

Precipitation seasonality (Bio_15) was the highest in Asia (27.6–152) (Figure 3d), as was the temperature seasonality (Bio_4) (see Figure 3a). However, the ranges of the variable changed, to some extent, to coincide in all regions, both with the EAB presence and in those where its presence had not been predicted. In points with EAB presence in European Russia and Ukraine, Bio_15 is from 17.6 in Klin to 36.5 in Miluvatka (Table S1), and in the territory, where MaxEnt does not predict invasion, this variable is from 14.9 in Evpatoria to 48,8 in Chernivtsi, is 25.9 in Bratislava and 46.4 in Prague.

Maximum temperature values of the warmest month (Bio_5) (July-August) in all compared groups of location vary within close limits. The highest maximum value was noted for America (35.1 °C), and the lowest—was for the European part, where the EAB appearance is not predicted (24.9 °C) (Figure 3d). At points with EAB presence in European Russia and Ukraine, Bio_5 was from 21.5 °C in Astrakhan to 29.2 °C in St. Petersburg, and in the regions where MaxEnt had not predicted invasion, this variable was from 22.9 °C in Lviv to 28.5 °C in Kherson (Table S1).

The mean temperature of the coldest quarter (Bio_11) (Figure 3e), as well as the min temperature of the coldest quarter (Bio_6) (see Figure 3b), was the lowest in Asia (average was −8.9, the minimum was −19.3 °C). In the groups of points with EAB presence in North America and the EAB-predicted territory for parts of Europe, the average values of Bio_11 were slightly different (−3.4 and −3.3 °C, respectively), although the range in North America was larger (−15.2–8.1 °C), than in EAB-predicted territory for parts of Europe (−5.7–2.5 °C). In the regions where EAB presence is not predicted by our model, the mean temperature of the coldest quarter is the highest (average −0.4, range −2–+1.1 °C). At points with EAB presence in European Russia and Ukraine, Bio_11 is from −8.8 °C in Michurinsk to −2.4 °C in Azov, and in the territory, where MaxEnt does not predict invasion, this variable is from −5.7 °C in Sumy to +2.5 °C in Simferopol (Table S1), and it is −0.3 in Prague (Table 7).

4. Discussion

EAB was found in Ukraine in 2019, but the presence of exit holes confirmed the invasion at least 2 years earlier [54]. EAB infested *F. excelsior* and *F. pennsylvanica* in Ukraine [18]. *Fraxinus excelsior* was one of the main forest-forming species in Ukraine and neighboring European countries [23,89], but in recent years, it has been weakened by ash dieback [90]. *F. pennsylvanica* has been widely used in landscaping and in roadside forest belts, along which EAB has quickly spread, both actively and passively, in different regions [8–10,13,14]. According to publications, EAB expansion rates have been up to 80 km/year in North America and up to 40 km/year in European Russia [37,91,92]. In Ukraine, for two years, EAB spread over more than 300 km from their entry point [19]. At this rate, in a few years, it will likely spread across Ukraine and invade neighboring European countries.

EAB distribution has been predicted using different approaches and data concerning environmental variables [27,29,39], import pathways via deciduous wood chips [32], host-tree spread [40], etc. Analyses have shown that in the area currently occupied by EAB, the AGDD10 was 714 °C in Asia, 705 °C in North America, and 711 °C in European Russia [11,37]. Furthermore, for heat availability, only the northern parts of Norway, Sweden, and Finland were not suitable for EAB [11]. We preferred the MaxEnt model [60–62,75,76] to test bioclimatic variables that characterize the temperature and rainfall for different parts of the year [63]. Sobek-Swant et al. [39] had predicted the potential distributions of

EAB using Bio_1 (mean annual temperature), Bio_11 (mean temperature of the coldest quarter), Bio_12 (annual precipitation), and Bio_19 (precipitation of coldest quarter), but the resulting predicted range failed to include some regions in China where EAB has been commonly observed. Liang and Fei [36] selected the minimum temperature of the coldest month (Bio_6), the maximum temperature of the warmest month (Bio_5), the annual temperature range (Bio_4), and the minimum temperature in June. The results suggested that the divergence between the invasion range of EAB and the distribution of ash in North America was likely to enlarge as climate change continues. In this case, many original ash stands could remain intact in the southern range.

Dang et al. [21] used the annual mean temperature (Bio_1), the maximum temperature of the warmest month (Bio_5), the precipitation of the warmest quarter (Bio_18), and the minimum temperature of the coldest month (Bio_6) to predict the potential distributions of EAB, and the annual mean temperature, the maximum temperature of the warmest month, and the precipitation of the driest month (Bio_14) to predict the suitability of potential areas for the susceptible host trees of EAB in China. They concluded that the inclusion of susceptible host-plant presence as a factor enabled more effective predictive modeling and risk assessment for biological invasions.

When choosing bioclimatic variables, we analyzed the geography of EAB distribution in the native (Asia) and invasive ranges (North America, European Russia, and Ukraine) (Table S1). We found that EAB was present in the study territory with nine climate types via Köppen–Geiger classification [72]: BSh—hot semiarid (central U.S.), BSk—cold semi-arid (Astrakhan), Cfa—temperate with hot summer (Hiroshima, Texas, Cincinnati, Azov), Cfb—temperate with warm summer (Colorado), Cwa—temperate with dry winter and hot summer (Tianjin), Dfa—continental with hot summer (Michigan, Svatove), Dfb—continental with warm summer (Yangkiaping, Manitoba, St. Petersburg, Moscow), Dwa—continental with dry winter and hot summer (Harbin, Changchun), and Dwb—continental with dry winter and warm summer (Far East of Russia). This testified to the high plasticity of EAB. At the same time, due to the diversity of climate types in these regions, the roles of particular climatic factors influencing the development and distribution of this pest could differ. Furthermore, the driest and wettest months, as well as the temperature in these months, differed significantly (see Table 5, Table 6 and Table S2). Therefore, in the same months, different EAB stages and instars could prevail and react differently to environmental factors, such as an excess or a lack of moisture.

In North America, adult emergence generally began between early May (southern Ohio) and mid-June (Central Michigan), peaked from mid-June to early July, and completed by early August [41,85]. In Tianjin (Asia), EAB emerged from early May to late June [3], and in European Russia, EAB emerged in early June, and the adults occurred from early June to early July [42]. In Michigan (North America), EAB emerged when AGDD10 was 275–325 °C [85]. At the same time, in Luhansk, EAB emergence was observed from June 14 to July 4 [67], which was 3 weeks later than expected, according to its AGDD10. Such an AGDD10 in Prague was estimated from 4 to 11 June.

An analysis of publications showed that all known foci of EAB were located in regions with pronounced seasonality. Therefore, the development of host plants and their pests has adapted to such changes. Ash foliage nutrition was essential for the maturation of EAB's reproductive system. Therefore, the earliest terms of adult emergence should coincide with the presence of sufficiently developed ash leaves. It was known that after the completion of pupal development, an adult would remain in the pupal chamber for several days before feeding on ash foliage for one week before mating and another two weeks after mating [2,3]. Therefore, the appearance of adults even three weeks before the leaves turn yellow would be risky. According to our data, in East Ukraine, ash leaves were sufficiently developed in the first half of May and turned yellow in the second half of August. Therefore, the last adults of EAB were found at the end of July.

The feeding of EAB larvae under the bark, similar to many other xylophagous beetles [67–69,83,84], was possible only during the growing season, when there was sap flow

in the host tree (that is, at temperatures above 10 °C). During this period, the duration of individual instars and stages of EAB depended primarily on temperature [43], although it could slow down due to low substrate moisture [54]. In regions with a sufficient heat supply, EAB developed by the 1-year cycle [41], and if the heat supply was insufficient, it developed according to the 2-year cycle [42]. In both cases, larvae would hibernate under the bark (once in a 1-year cycle, twice in the 2-year cycle) with diverse instar composition [6,43]. In East Ukraine, EAB had two cohorts, where one part of the population was a progeny of the females that swarmed and oviposited earlier, and another part was a progeny of the females that oviposited later in the same summer [54].

According to the long-term data [73], a stable temperature transition through 10 °C in spring in Kharkiv was from April 13 to 24 and in autumn from September 9 to 25, and the AGDD10 was 1600–1900 °C. The duration of this period was 6–7 months in East Ukraine, and 5 months in the central and western parts of the country. In the steppe zone of Ukraine, it was from 14–17 April to 6–19 October; in the forest-steppe zone from 17–23 April to 29 September–5 October; and in the forest zone (Polissya) from 22–23 April to 1–10 October [93].

Taking into account these features of EAB development, we used all 19 bioclimatic variables to predict its spread. MaxEnt predicted the potential spread of EAB in the east of Ukraine with high model accuracy (Table 6, Tables S3 and S4). Six variables had the highest contribution to the model (95.19% together), particularly, the temperature seasonality (Bio_4), the minimum temperature of the coldest month (Bio_6), the precipitation of the coldest quarter (Bio_19), the precipitation seasonality (Bio_15), the maximal temperature of the warmest month (Bio_5), and the mean temperature of the coldest quarter (Bio_11).

Three of these variables (Bio_4, Bio_5, Bio_6) matched with Liang and Fei [36], two variables (Bio_5, Bio_6) with Dang et al. [21], and two other variables (Bio_11, Bio_19)—with results from Sobek-Swant et al. [39].

The mapping of the predicted range of EAB showed the highest risk of its spread in the Luhansk, Kharkiv, and Donetsk regions (Figure 2). On the one hand, these areas are the nearest to the first EAB entrance to Ukraine and have more similar climatic conditions (see Tables S1 and S2, Figure 2). On the other hand, small spots of possible EAB foci were revealed in the central and western regions of Ukraine, in Romania, and in Poland (see Figure 2).

The precipitation in the coldest quarter of the year (Bio_19) in the area with EAB presence was slightly higher than in the area where its presence had not been predicted. The precipitation during the cold season (snow) could have had a positive effect on EAB survival by softening the effect of frost. However, in the western part of the studied region, within similar latitudes (Lviv and Prague), the frost (Bio_6) was less than in Kharkiv, with a high probability of EAB invasion (see Table 7 and Table S2). However, the MaxEnt modeling using bioclimatic variables showed a high risk of EAB invasion only in the nearest locations from the current foci.

We attempted to compare the individual variables at points where invasion had been predicted and where its probability had been low. An analysis of previous publications showed that not all forecasts had been realized. Therefore, the complex prognosis of EAB spread in North America that considered forest types, the number of ash trees, the distance between the trees, and the location of roads [94] had not been realized [15]. Orlova-Bienkowskaja and Bieńkowski [15] predicted that by 2022, EAB could be detected in the eastern parts of Belarus, Ukraine, Estonia, Latvia, and Lithuania. As of 2022, within European Russia, EAB had spread to the north, south, and east, but had not yet been found in Baltic countries and Belarus, which were closer to the distribution points of EAB in Russia.

We did not have enough information to explain why, according to climatic parameters, EAB had not spread to the west. It was also difficult to explain why EAB spread more to the east than to the west in European Russia, just as it was difficult to explain why *Anoplophora glabripennis* (Motschulsky, 1853) [95] and *Agrilus anxius* Gory, 1841 [96] had not yet spread to the east of Europe, despite the presence of available tree species.

Using seven variables (the degree of EAB infestation, the host tree species, age, size, habitat, latitude, and elevation), it was demonstrated that planting susceptible non-native host plants could promote outbreaks of a native insect pest in its native range [64]. In Ukraine, *F. excelsior* was common in the forest, as well as *F. pennsylvanica* in the forest belts and urban stands [23,89], and EAB inhabited both tree species there [18]. However, even within the same forest, uninhabited plots and trees were present.

An analysis of existing publications [3,6,50,52,87,97] showed that the attractiveness of trees for EAB and the rate of its survival and development depended on many factors related to the landscape, the location of stands, their structures, and the health of the trees. Many of these factors determined the microclimate, the performance of which differed from that of weather stations. According to previous publications, EAB preferred trees with sparse crowns for mating and laying eggs. Its larvae developed longer in healthier trees [50,87]. The population density, the development rate, and the survival of individuals were higher in more illuminated trees [6], particularly at the forest edges [3,97]. These traits were higher at optimal bark thickness (1.5–5.0 mm [6]), which was coarse enough to protect larvae and pupae from desiccation, extreme temperatures, predators, and parasites. The population density of EAB depended on the age and the density of the stands [52].

Our modeling of EAB spread in Ukraine and westward was the first step. The set of points marking EAB's actual presence in Ukraine was still quite small. Therefore, the reasons for EAB absence even in neighboring Donetsk were not clear. To improve forecasting accuracy, we plan to add the data on host-plant distribution, stand structure determining the microclimate, as well as the localization of roads along which the pest can spread passively, to the bioclimatic variables.

5. Conclusions

1. All known foci of EAB were located in regions with a pronounced seasonality. Therefore, the development of the host tree and the pest had adapted to such changes. EAB adults emerge after the ash foliage developed, and the last specimens were found before the foliage began to turn yellow. Larvae feeding and development under the bark occurred during a period with temperatures above 10 °C.
2. When constructing the EAB range model for Ukraine and westward, 6 bioclimatic variables had a cumulative contribution of 95.19%, particularly Bio_4 (the variation of temperature over a given year), Bio_6 (the minimal temperature of the coldest month), Bio_19 (the precipitation of the coldest quarter), Bio_15 (the precipitation seasonality), Bio_5 (the monthly mean of daily high temperatures for the hottest month), and Bio_11 (the mean temperatures during the coldest 3 months of the year). The model predicted a high probability of EAB spread in East Ukraine. The EAB spread would exceed 87% of the area in Luhansk, 48% in Kharkiv, and 32% in Donetsk.
3. The ranges of the bioclimatic variables in different regions of EAB presence showed the high ecological plasticity of this pest. However, its spread was not predicted using MaxEnt for some points with similar bioclimatic variables. To improve the forecasting accuracy, it could be necessary to add the data on host-plant distribution, the stand structure determining the microclimate, as well as the localization of roads along which the pest can spread passively, to the bioclimatic variables.

Supplementary Materials: The following supporting information can be downloaded at: https://www.mdpi.com/article/10.3390/f14040736/s1, Table S1: Localities in Asia, North America, and Europe, with EAB detected by October 2022, and the localities in Ukraine and Europe for EAB prediction; Table S2: Mean monthly temperature and precipitation (1989–2019) for selected points on different continents with EAB presence (with 1-year and 2-year cycles) and absence; Table S3: Response curves of bioclimatic variables used for MaxEnt modeling of EAB spread; Table S4: Results of MaxEnt modeling of EAB spread.

Author Contributions: Conceptualization, V.M. and O.B.; methodology, V.M. and O.B.; validation, V.M. and O.B.; formal analysis and investigation, Y.S., K.D. and T.K.; data curation, K.D. and Y.S.;

writing—original draft preparation, V.M. and O.B.; writing—review and editing, V.M. and K.D.; visualization, O.B.; supervision, V.M. and J.H. All authors have read and agreed to the published version of the manuscript.

Funding: This research was funded by Funding: Project EVA 4.0 Advanced Research Supporting the Forestry and Wood-Processing Sector's Adaptation to Global Change and the Fourth Industrial Revolution, CZ.02.1.01/0.0/0.0/16_019/0000803 Czech University of Life Sciences Prague. K.D. was funded by the Swedish Foundation for Strategic Research (SSF) project UKR22-0060, Knut and Alice Wallenberg's foundation project KAW 2022.0211.

Institutional Review Board Statement: Not applicable.

Informed Consent Statement: Not applicable.

Data Availability Statement: Data are available upon e-mail request to the corresponding author.

Conflicts of Interest: The authors declare no conflict of interest.

References

1. Baranchikov, Y.N.; Seraya, L.G.; Grinash, M.N. All European ash species are susceptible to emerald ash borer *Agrilus planipennis* Fairmaire (Coleoptera: Buprestidae)—A Far Eastern invader. *Sib. For. J.* **2014**, *6*, 80–85.
2. Haack, R.A.; Baranchikov, Y.; Bauer, L.S.; Poland, T.M. Emerald ash borer biology and invasion history. In *Biology and Control of Emerald Ash Borer*; Van Driesche, R.G., Reardon, R.C., Eds.; FHTET-2014-09 Department of Agriculture, Forest Service, Forest Health Technology Enterprise Team: Morgantown, WV, USA, 2015; Chapter 1; pp. 1–13.
3. Wang, X.Y.; Yang, Z.Q.; Gould, J.R.; Zhang, Y.N.; Liu, G.J.; Liu, E.S. The biology and ecology of the emerald ash borer, *Agrilus planipennis*, in China. *J. Insect Sci.* **2010**, *10*, 128. [CrossRef] [PubMed]
4. Herms, D.A.; McCullough, D.G. Emerald ash borer invasion of North America: History, biology, ecology, impacts, and management. *Annu. Rev. Entomol.* **2014**, *59*, 13–30. [CrossRef] [PubMed]
5. Haack, R.A.; Jendek, E.; Liu, H.; Marchant, K.R.; Petrice, T.R.; Poland, T.M.; Ye, H. The emerald ash borer: A new exotic pest in North America. *Newsl. Mich. Entomol. Soc.* **2002**, *47*, 1–5.
6. Timms, L.L.; Smith, S.M.; De Groot, P. Patterns in the within-tree distribution of the emerald ash borer *Agrilus planipennis* (Fairmaire) in young, green-ash plantations of south-western Ontario, Canada. *Agric. For. Entomol.* **2006**, *8*, 313–321. [CrossRef]
7. Orlova-Bienkowskaja, M.J. European range of the emerald ash borer *Agrilus planipennis* (Coleoptera: Buprestidae) is expanding: The pest destroys ashes in the northwest of Moscow Oblast and in part of Tver Oblast. *Russ. J. Biol. Invasions* **2014**, *5*, 32–37. [CrossRef]
8. Orlova-Bienkowskaja, M.J. Ashes in Europe are in danger: The invasive range of *Agrilus planipennis* in European Russia is expanding. *Biol. Invasions* **2014**, *16*, 1345–1349. [CrossRef]
9. Selikhovkin, A.V.; Popovichev, B.G.; Mandelshtam, M.Y.; Vasaitis, R.; Musolin, D.L. The frontline of invasion: The current Northern limit of the invasive range of Emerald ash borer, *Agrilus planipennis* Fairmaire (Coleoptera: Buprestidae), in European Russia. *Balt. For.* **2017**, *23*, 309–315.
10. Selikhovkin, A.V.; Popovichev, B.G.; Merkuryev, S.A.; Volkovitsh, M.G.; Vasaitis, R.; Musolin, D.L. Invasive populations of Emerald ash borer *Agrilus planipennis* Fairmaire, 1888 (Coleoptera: Buprestidae) in Saint Petersburg, Russia: A "Hitchhiker"? *Insects* **2021**, *13*, 191. [CrossRef]
11. Orlova-Bienkowskaja, M.J.; Bieńkowski, A.O. Low heat availability could limit the potential spread of the Emerald ash borer to Northern Europe (Prognosis Based on Growing Degree Days per Year). *Insects* **2022**, *13*, 52. [CrossRef]
12. Orlova-Bienkowskaja, M.J.; Bieńkowski, A.O. Southern range expansion of the Emerald ash borer, *Agrilus planipennis*, in Russia threatens ash and olive trees in the Middle East and Southern Europe. *Forests* **2022**, *13*, 541. [CrossRef]
13. Shchurov, V.I.; Zamotailov, A.S. The first findings of the emerald ash borer *Agrilus planipennis* Fairmaire, 1888 (Coleoptera: Buprestidae) in the Krasnodar krai. In Proceedings of the XXIV International Scientific Conference "Biological diversity of the Caucasus and Southern Russia", Magas, Russia, 17–20 November 2022; ALEF Publishing House: Makhachkala, Russia, 2022; pp. 558–565, ISBN 978-5-00212-129-8.
14. Musolin, D.L.; Selikhovkin, A.V.; Peregudova, E.Y.; Popovichev, B.G.; Mandelshtam, M.Y.; Baranchikov, Y.N.; Vasaitis, R. North-Westward expansion of the invasive range of Emerald ash borer, *Agrilus planipennis* Fairmaire (Coleoptera: Buprestidae) towards EU: From Moscow to Saint Petersburg. *Forests* **2021**, *12*, 502. [CrossRef]
15. Orlova-Bienkowskaja, M.J.; Bieńkowski, A.O. Modeling long-distance dispersal of emerald ash borer in European Russia and prognosis of spread of this pest to neighboring countries within next 5 years. *Ecol. Evol.* **2018**, *8*, 9295–9304. [CrossRef]
16. Drogvalenko, A.N.; Orlova-Bienkowskaja, M.J.; Bienkowski, A.O. Record of the Emerald ash borer (*Agrilus planipennis*) in Ukraine is confirmed. *Insects* **2019**, *10*, 338. [CrossRef]
17. Orlova-Bienkowskaja, M.J.; Drogvalenko, A.N.; Zabaluev, I.A.; Sazhnev, A.S.; Peregudova, E.Y.; Mazurov, S.G.; Komarov, E.V.; Struchaev, V.V.; Martynov, V.V.; Nikulina, T.V.; et al. Current range of *Agrilus planipennis* Fairmaire, an alien pest of ash trees, in European Russia and Ukraine. *Ann. For. Sci.* **2020**, *77*, 1–14. [CrossRef]

18. Meshkova, V.L.; Kucheryavenko, T.V.; Skrylnik, Y.E.; Zinchenko, O.V.; Borysenko, A.I. Beginning of the spread of *Agrilus planipennis* Fairmaire (Coleoptera: Buprestidae) on the territory of Ukraine. *Proc. St. Petersburg For. Tech. Acad.* **2021**, *236*, 163–184.
19. Meshkova, V.L.; Skrylnyk, Y.E.; Terekhova, V.V.; Kucheryavenko, T.V. Emerald ash borer (*Agrilus planipennis*) in Kharkiv Region. In Proceedings of the International Scientific and Practical Conference Modern Problems of Forestry and Ecology: Ways of Solution, Zhytomyr: Polissya National University, Zhytomyr, Ukraine, 7–8 October 2021; pp. 125–126, ISBN 978-617-7684-65-6.
20. Poland, T.M.; Chen, Y.; Koch, J.; Pureswaran, D. Review of the emerald ash borer (Coleoptera: Buprestidae), life history, mating behaviours, host plant selection, and host resistance. *Can. Entomol.* **2015**, *147*, 252–262. [CrossRef]
21. Dang, Y.Q.; Zhang, Y.L.; Wang, X.Y.; Xin, B.; Quinn, N.F.; Duan, J.J. Retrospective analysis of factors affecting the distribution of an invasive wood-boring insect using native range data: The importance of host plants. *J. Pest Sci.* **2021**, *94*, 981–990. [CrossRef]
22. Davydenko, K.; Skrylnyk, Y.; Borysenko, O.; Menkis, A.; Vysotska, N.; Meshkova, V.; Olson, A.; Elfstrand, M.; Vasaitis, R. Invasion of Emerald ash borer *Agrilus planipennis* and ash dieback pathogen *Hymenoscyphus fraxineus* in Ukraine–A concerted action. *Forests* **2022**, *13*, 789. [CrossRef]
23. FRAXIGEN. *Ash Species in Europe: Biological Characteristics and Practical Guidelines for Sustainable Use*; Oxford Forestry Institute, University of Oxford: Oxford, UK, 2005; p. 128. ISBN 085074.163.7.
24. Vasaitis, R.; Enderle, R. *Dieback of European Ash (Fraxinus spp.)–Consequences and Guidelines for Sustainable Management*; Swedish University of Agricultural Sciences: Uppsala, Sweden, 2017; p. 320. Available online: http://www.slu.se/globalassets/ew/org/inst/mykopat/forskning/stenlid/dieback-of-european-ash.pdf (accessed on 31 August 2021).
25. Enderle, R.; Stenlid, J.; Vasaitis, R. An overview of ash (*Fraxinus* spp.) and ash dieback disease in Europe. *CAB Rev.* **2019**, *14*, 025. [CrossRef]
26. Meshkova, V.; Samoday, V.; Davydenko, K. Ash dieback and contributing factors of forest weakening in provenance tests in the Sumy region. *Cent. Eur. For. J.* **2021**, *67*, 113–121. [CrossRef]
27. BenDor, T.K.; Metcalf, S.S.; Fontenot, L.E.; Sangunett, B.; Hannon, B. Modeling the spread of the emerald ash borer. *Ecol. Model.* **2006**, *197*, 221–236. [CrossRef]
28. Muirhead, J.R.; Leung, B.; van Overdijk, C.; Kelly, D.W.; Nandakumar, K.; Marchant, K.R.; MacIsaac, H.J. Modelling local and long-distance dispersal of invasive emerald ash borer *Agrilus planipennis* (Coleoptera) in North America. *Divers. Distrib.* **2006**, *12*, 71–79. [CrossRef]
29. Prasad, A.M.; Iverson, L.R.; Peters, M.P.; Bossenbroek, J.M.; Matthews, S.N.; Sydnor, T.D.; Schwartz, M.W. Modeling the invasive emerald ash borer risk of spread using a spatially explicit cellular model. *Landsc. Ecol.* **2010**, *25*, 353–369. [CrossRef]
30. Yemshanov, D.; Koch, F.H.; Lyons, D.B.; Ducey, M.; Koehler, K. A dominance-based approach to map risks of ecological invasions in the presence of severe uncertainty. *Divers. Distrib.* **2012**, *18*, 33–46. [CrossRef]
31. Yemshanov, D.; Haight, R.G.; Koch, F.H.; Lu, B.; Venette, R.; Lyons, D.B.; Scarr, T.; Ryall, K. Optimal allocation of invasive species surveillance with the maximum expected coverage concept. *Divers. Distrib.* **2015**, *21*, 1349–1359. [CrossRef]
32. Flø, D.; Krokene, P.; Økland, B. Invasion potential of *Agrilus planipennis* and other *Agrilus* beetles in Europe: Import pathways of deciduous wood chips and MaxEnt analyses of potential distribution areas. *EPPO Bull.* **2015**, *45*, 259–268. [CrossRef]
33. Orlova-Bienkowskaja, M.J.; Bieńkowski, A.O. Minimum winter temperature as a limiting factor of the potential spread of *Agrilus planipennis*, an alien pest of ash trees, in Europe. *Insects* **2020**, *11*, 258. [CrossRef]
34. Liebhold, A.M.; Brockerhoff, E.G.; Kalisz, S.; Nuñez, M.A.; Wardle, D.A.; Wingfield, M.J. Biological invasions in forest ecosystems. *Biol. Invasions* **2017**, *19*, 3437–3458. [CrossRef]
35. Liu, H.; Bauer, L.S.; Miller, D.L.; Zhao, T.; Gao, R.; Song, L.; Luan, Q.; Jin, R.; Gao, C. Seasonal abundance of *Agrilus planipennis* (Coleoptera: Buprestidae) and its natural enemies *Oobius agrili* (Hymenoptera: Encyrtidae) and *Tetrastichus planipennisi* (Hymenoptera: Eulophidae) in China. *Biol. Control* **2007**, *42*, 61–71. [CrossRef]
36. Liang, L.; Fei, S. Divergence of the potential invasion range of emerald ash borer and its host distribution in North America under climate change. *Clim. Chang.* **2014**, *122*, 735–746. [CrossRef]
37. Webb, C.R.; Mona, T.; Gilligan, C.A. Predicting the potential for spread of emerald ash borer (*Agrilus planipennis*) in Great Britain: What can we learn from other affected areas? *Plants People Planet* **2021**, *3*, 402–413. [CrossRef]
38. Sobek-Swant, S.; Crosthwaite, J.C.; Lyons, D.B.; Sinclair, B.J. Could phenotypic plasticity limit an invasive species? Incomplete reversibility of mid-winter deacclimation in emerald ash borer. *Biol. Invasions* **2012**, *14*, 115–125. [CrossRef]
39. Sobek-Swant, S.; Kluza, D.A.; Cuddington, K.; Lyons, D.B. Potential distribution of emerald ash borer: What can we learn from ecological niche models using Maxent and GARP? *For. Ecol. Manag.* **2012**, *281*, 23–31. [CrossRef]
40. Valenta, V.; Moser, D.; Kuttner, M.; Peterseil, J.; Essl, F. A high-resolution map of emerald ash borer invasion risk for southern central Europe. *Forests* **2015**, *6*, 3075–3086. [CrossRef]
41. Discua Duarte, S.A. Characterizing Prepupal Diapause and Adult Emergence Phenology of Emerald Ash Borer. Doctoral Dissertation, The Ohio State University, Columbus, OH, USA, 2013.
42. Orlova-Bienkowskaja, M.J.; Bienkowski, A.O. The life cycle of the emerald ash borer *Agrilus planipennis* in European Russia and comparisons with its life cycles in Asia and North America. *Agric. For. Entomol.* **2016**, *18*, 182–188. [CrossRef]
43. Wei, X.I.A.; Wu, Y.U.N.; Reardon, R.; Sun, T.H.; Lu, M.I.N.; Sun, J.H. Biology and damage traits of emerald ash borer (*Agrilus planipennis* Fairmaire) in China. *Insect Sci.* **2007**, *14*, 367–373. [CrossRef]
44. Vermunt, B.; Cuddington, K.; Sobek-Swant, S.; Crosthwaite, J. Cold temperature and emerald ash borer: Modelling the minimum under-bark temperature of ash trees in Canada. *Ecol. Model.* **2012**, *235*, 19–25. [CrossRef]

45. Brown-Rytlewski, D.; Wilson, M. Tracking the emergence of emerald ash borer adults. In *Emerald Ash Borer Research and Technology Development Meeting*; Mastro, V., Reardon, R., Eds.; U.S. Department of Agriculture, Forest Service: Morgantown, WV, USA, 2005; pp. 13–14.
46. Cappaert, D.; McCullough, D.G.; Poland, T.M.; Siegert, N.W. Emerald ash borer in North America: A research and regulatory challenge. *Am. Entomol.* **2005**, *51*, 152–165. [CrossRef]
47. Christianson, L.D.; Venette, R.C. Modest effects of host on the cold hardiness of emerald ash borer. *Forests* **2018**, *9*, 346. [CrossRef]
48. Crosthwaite, J.C.; Sobek, S.; Lyons, D.B.; Bernards, M.A.; Sinclair, B.J. The over-wintering physiology of the emerald ash borer, *Agrilus planipennis* Fairmaire (Coleoptera: Buprestidae). *J. Insect Physiol.* **2011**, *57*, 166–173. [CrossRef] [PubMed]
49. Duan, J.J.; Schmude, J.M.; Larson, K.M. Effects of low temperature exposure on diapause, development, and reproductive fitness of the emerald ash borer (Coleoptera: Buprestidae): Implications for voltinism and laboratory rearing. *J. Econ. Entomol.* **2021**, *114*, 201–208. [CrossRef]
50. Duan, J.J.; Watt, T.; Taylor, P.; Larson, K.; Lelito, J.P. Effects of ambient temperature on egg and larval development of the invasive emerald ash borer (Coleoptera: Buprestidae): Implications for laboratory rearing. *J. Econ. Entomol.* **2013**, *106*, 2101–2108. [CrossRef] [PubMed]
51. Duell, M.E.; Gray, M.T.; Roe, A.D.; MacQuarrie, C.J.; Sinclair, B.J. Plasticity drives extreme cold tolerance of emerald ash borer (*Agrilus planipennis*) during a polar vortex. *Curr. Res. Insect Sci.* **2022**, *2*, 100031. [CrossRef] [PubMed]
52. Jennings, D.E.; Taylor, P.B.; Duan, J.J. The mating and oviposition behavior of the invasive emerald ash borer (*Agrilus planipennis*), with reference to the influence of host tree condition. *J. Pest Sci.* **2014**, *87*, 71–78. [CrossRef]
53. Petrice, T.R.; Haack, R.A. Can Emerald ash borer, *Agrilus planipennis* (Coleoptera: Buprestidae), emerge from logs two summers after infested trees are cut? *Great Lakes Entomol.* **2007**, *40*, 92–95.
54. Kucheryavenko, T.V.; Skrylnik, Y.E.; Davydenko, K.V.; Zinchenko, O.V.; Meshkova, V.L. The first data on the biological characteristics of *Agrilus planipennis* Fairmare, 1988 (Coleoptera: Buprestidae) in Ukraine. *Ukrainian Entomol. J.* **2020**, *18*, 58–66. [CrossRef]
55. Holusa, J.; Holuša, J.; Kaláb, O. Using Habitat-Suitability Models to Improve Management of the Mole Cricket (Gryllotalpa Gryllotalpa) in Gardens and Forest Nurseries. Available online: https://ssrn.com/abstract=4034077 (accessed on 31 August 2021). [CrossRef]
56. Zielińska, A.; Lis, B. Evaluation of the possibilities of potential expansion of the oak lace bug *Corythucha arcuata* (Say, 1832), an invasive species of Tingidae (Hemiptera: Heteroptera), into the territory of Poland. *Heteroptera Pol.–Acta Faun.* **2020**, *14*, 175–180.
57. Wang, C.-J.; Wang, R.; Yu, C.-M.; Dang, X.-P.; Sun, W.-G.; Li, Q.-F.; Wang, X.-T.; Wan, J.-Z. Risk assessment of insect pest expansion in alpine ecosystems under climate change. *Pest Manag. Sci.* **2021**, *77*, 3165–3178. [CrossRef]
58. Warren, D.L.; Seifert, S.N. Ecological niche modeling in Maxent: The importance of model complexity and the performance of model selection criteria. *Ecol. Appl.* **2011**, *21*, 335–342. [CrossRef]
59. Phillips, S.J.; Anderson, R.P.; Schapire, R.E. Maximum entropy modeling of species geographic distributions. *Ecol. Model.* **2006**, *190*, 231–259. [CrossRef]
60. Elith, J.; Graham, C.H. Do They? How Do They? WHY Do They Differ? On Finding Reasons for Differing Performances of Species Distribution Models. *Ecography* **2009**, *32*, 66–77. Available online: https://www.jstor.org/stable/30244651 (accessed on 4 August 2022). [CrossRef]
61. Fitzgibbon, A.; Pisut, D.; Fleisher, D. Evaluation of Maximum Entropy (Maxent) machine learning model to assess relationships between climate and corn suitability. *Land* **2022**, *11*, 1382. [CrossRef]
62. Olivera, L.; Minghetti, E.; Montemayor, S.I. Ecological niche modeling (ENM) of *Leptoglossus clypealis* a new potential global invader: Following in the footsteps of *Leptoglossus occidentalis*? *Bull. Entomol. Res.* **2020**, *111*, 289–300. [CrossRef]
63. O'Donnell, M.S.; Ignizio, D.A. *Bioclimatic Predictors for Supporting Ecological Applications in the Conterminous United States*; Data Series 691; U.S. Geological Survey: Reston, VA, USA, 2012. Available online: https://pubs.usgs.gov/ds/691/ds691.pdf (accessed on 10 August 2022).
64. Dang, Y.; Wei, K.; Wang, X.; Duan, J.J.; Jennings, D.E.; Poland, T.M. Introduced plants induce outbreaks of a native pest and facilitate invasion in the plants' native range: Evidence from the emerald ash borer. *J. Ecol.* **2022**, *110*, 593–604. [CrossRef]
65. Emerald Ash Borer Informative Network. Available online: http://www.emeraldashborer.info/ (accessed on 3 November 2022).
66. GBIF.org GBIF Occurrence Download: *Agrilus planipennis*, Canada and the USA. Available online: https://www.gbif.org/occurrence/download/0034381-210914110416597 (accessed on 23 October 2021).
67. Kucheryavenko, T.V. Dynamics of emergence of emerald ash borer *Agrilus planipennis* beetles in Luhansk region. *For. For. Melior.* **2022**, *140*, 64–70. [CrossRef]
68. Chernyavska, O.M. Inhabitation of oak stumps by *Agrilus biguttatus* F. (Buprestidae). *For. For. Melior.* **2006**, *109*, 261–264.
69. Meshkova, V.L.; Kukina, O.M. *Duration of Development of Agrilus biguttatus F.*; Series «Phytopathology and Entomology»; The Bulletin of Kharkiv National Agrarian University: Dokuchaievske, Ukraine, 2008; Volume 8, pp. 102–105.
70. Reed, K.; Denman, S.; Leather, S.R.; Forster, J.; Inward, D.J. The lifecycle of *Agrilus biguttatus*: The role of temperature in its development and distribution, and implications for Acute Oak Decline. *Agric. For. Entomol.* **2018**, *20*, 334–346. [CrossRef]
71. Copernicus Climate Change Service (C3S): C3S ERA5-Land Reanalysis. Copernicus Climate Change Service. Available online: https://cds.climate.copernicus.eu/cdsapp#!/home (accessed on 12 September 2022).

72. Peel, M.C.; Finlayson, B.L.; McMahon, T.A. Updated world map of the Köppen-Geiger climate classification. *Hydrol. Earth Syst. Sci.* **2007**, *11*, 1633–1644. [CrossRef]
73. Zepner, L.; Karrasch, P.; Wiemann, F.; Bernard, L. ClimateCharts.net–an interactive climate analysis web platform. *Int. J. Digit. Earth* **2020**, *14*, 338–356. [CrossRef]
74. Meshkova, V.L. *Seasonal Development of Foliage Browsing Insects*; Novoe Slovo: Kharkov, Ukraine, 2009; pp. 1–396. ISBN 978-966-2046-69-4.
75. Phillips, S.J. 2014 A Brief Tutorial on Maxent [Internet]. Available online: http://www.cs.princeton.edu/~schapire/maxent/ (accessed on 23 June 2022).
76. Phillips, S.J.; Dudik, M.; Schapire, R.E. Maxent Software for Modeling Species Niches and Distributions. Version 3.4.4. Available online: http://biodiversityinformatocs.amnh.org/open_source/maxent/MaxEnt (accessed on 1 December 2022).
77. Fick, S.E.; Hijmans, R.J. WorldClim 2: New 1-Km Spatial Resolution Climate Surfaces for Global Land Areas. *Int. J. Climatol.* **2017**, *37*, 4302–4315. Available online: https://www.worldclim.org/data/worldclim21.html (accessed on 23 September 2022). [CrossRef]
78. Hijmans, R.J.; Cameron, S.E.; Parra, J.L.; Jones, P.G.; Jarvis, A. Very high resolution interpolated climate surfaces for global land areas. *Int. J. Climatol.* **2005**, *25*, 1965–1978. [CrossRef]
79. QGIS 3.28.1. Available online: https://qgis.org/en/site/ (accessed on 23 September 2022).
80. Van Erkel, A.R.; Peter, M. Receiver operating characteristic (ROC) analysis: Basic principles and applications in radiology. *Eur. J. Radiol.* **1998**, *27*, 88–94. [CrossRef] [PubMed]
81. Hammer, O.; Harper, D.A.T.; Ryan, P.D. PAST: Paleontological statistics software package for education and data analysis. *Palaeontol. Electron.* **2001**, *4*, 9.
82. Marshall, J.M.; Miller, M.A.; Lelito, J.P.; Storer, A.J. Latitudinal variation in body size of *Agrilus planipennis* and relationship with fecundity. *Agric. For. Entomol.* **2013**, *15*, 294–300. [CrossRef]
83. Meshkova, V.L.; Kochetova, A.I.; Skrylnik, Y.Y.; Zinchenko, O.V. Seasonal development of the timberman beetle *Acanthocinus aedilis* (Linnaeus, 1758) (Coleoptera: Cerambycidae) in the North-Eastern Steppe of Ukraine. *Kharkov Entomol. Soc. Gaz.* **2017**, *25*, 40–44. Available online: http://entomology.kharkiv.ua/index.php/KhESG/article/view/26 (accessed on 1 December 2022).
84. Meshkova, V.L.; Skrylnik, Y.Y.; Zinchenko, O.V.; Kochetova, A.I. Seasonal development of the pine sawyer beetle (*Monochamus galloprovincialis*) in the north-eastern steppe of Ukraine. *For. For. Melior.* **2017**, *130*, 223–230. Available online: http://forestry-forestmelioration.org.ua/index.php/journal/article/view/102/90 (accessed on 1 December 2022).
85. Poland, T.M.; McCullough, D.G.; Anulewicz, A.C. Evaluation of an artificial trap for *Agrilus planipennis* (Coleoptera: Buprestidae) incorporating olfactory and visual cues. *J. Econ. Entomol.* **2011**, *104*, 517–531. [CrossRef]
86. Chen, I.C.; Hill, J.K.; Ohlemüller, R.; Roy, D.B.; Thomas, C.D. Rapid range shifts of species associated with high levels of climate warming. *Science* **2011**, *333*, 1024–1026. [CrossRef]
87. Tluczek, A.R.; McCullough, D.G.; Poland, T.M. Influence of host stress on emerald ash borer (Coleoptera: Buprestidae) adult density, development, and distribution in *Fraxinus pennsylvanica* trees. *Environ. Entomol.* **2011**, *40*, 357–366. [CrossRef]
88. Canelles, Q.; Aquilué, N.; James, P.; Lawler, J.; Brotons, L. Global review on interactions between insect pests and other forest disturbances. *Landsc. Ecol.* **2021**, *36*, 945–972. [CrossRef]
89. Tkach, V.; Rumiantsev, M.; Luk'yanets, V.; Kobets, O.; Pozniakova, S.; Obolonyk, I.; Sydorenko, S. Common ash (*Fraxinus excelsior* L.) in Ukrainian forests and its successful natural regeneration. *For. Stud. Metsanduslikud Uurim.* **2020**, *73*, 26–42, ISSN 1406–9954. Available online: http://mi.emu.ee/forestry.studies (accessed on 1 December 2022). [CrossRef]
90. Davydenko, K.V.; Borysova, V.; Shcherbak, O.; Kryshtop, Y.; Meshkova, V. Situation and perspectives of European ash (*Fraxinus* spp.) in Ukraine: Focus on eastern border. *Balt. For.* **2019**, *25*, 193–202. [CrossRef]
91. Valenta, V.; Moser, D.; Kapeller, S.; Essl, F. A new forest pest in Europe: A review of Emerald ash borer (*Agrilus planipennis*) invasion. *J. Appl. Entomol.* **2017**, *141*, 507–526. [CrossRef]
92. Volkovitsh, M.G.; Bieńkowski, A.O.; Orlova-Bienkowskaja, M.J. Emerald ash borer approaches the borders of the European Union and Kazakhstan and is confirmed to infest European ash. *Forests* **2021**, *12*, 691. [CrossRef]
93. Adamenko, T.I.; Kulbida, M.I.; Prokopenko, A.L. *Agroclimatic Guide for the Territory of Ukraine*; PP Galagodza, R.S.: Kamianets-Podilskyi, Ukraine, 2011; pp. 1–108.
94. Iverson, L.R.; Prasad, A.; Bossenbroek, J.; Sydnor, D.; Schwartz, M.W. Modeling potential movements of the emerald ash borer: The model framework. In *Advances in Threat Assessment and Their Application to Forest and Rangeland Management*; Pye, J., Rauscher, H., Sands, Y., Lee, D., Beatty, J., Eds.; Gen. Tech. Rep. PNW-802; Department of Agriculture, Forest Service, Pacific Northwest and Southern Research Stations: Portland, OR, USA, 2010; pp. 581–597.
95. Yang, C.; Zhan, Z.; Zong, S.; Ren, L. The relationship between landscape patterns and populations of Asian longhorned beetles. *Forests* **2022**, *13*, 1981. [CrossRef]

96. Evans, H.F.; Williams, D.; Hoch, G.; Loomans, A.; Marzano, M. Developing a European Toolbox to manage potential invasion by emerald ash borer (*Agrilus planipennis*) and bronze birch borer (*Agrilus anxius*), important pests of ash and birch. *For. Int. J. For. Res.* **2020**, *93*, 187–196. [CrossRef]
97. Caitano, B.; Chaves, T.P.; Dodonov, P.; Delabie, J.H.C. Edge effects on insects depend on life history traits: A global meta-analysis. *J. Insect Conserv.* **2020**, *24*, 233–240. [CrossRef]